Molecular Cloning of *sodB* Gene from *Vibrio alginolyticus* HY9901 and Its Bioinformatics Analysis

Shuai YANG[1,2△], Yingying JIANG[1,2△], Haiyun FENG[1,2], Weijie ZHANG[1,2], Na WANG[3], Xiaonan LU[4], Huanying PANG[1,2*]

1. Fisheries College, Guangdong Ocean University, Zhanjiang 524025, China; 2. Guangdong Provincial Key Laboratory of Aquatic Animal Disease Control and Healthy Culture & Key Laboratory of Control for Diseases of Aquatic Economic Animals of Guangdong Higher Education Institutes, Zhanjiang 524025, China; 3. Chinese Academy of Inspection and Quarantine, Beijing, 100176, China; 4. Department of Food Science and Agricultural Chemistry, Faculty of Agricultural and Environmental Sciences, McGill University, Sainte-Anne-de-Bellevue H9X 3V9, Canada

Abstract *Vibrio alginolyticus* is a zoonotic bacterium. A pair of specific primers was designed using the *sodB* gene sequence of *Vibrio alginolyticus* HY9901 in order to amplify the full length of the gene by PCR. The results indicated that the total length of the *sodB* gene was 585 bp and that it could encode 194 amino acids. The predicted amino acid sequence derivation indicated that the molecular weight of the protein was approximately 21.56 kDa, with an isoelectric point of 4.95. Upon prediction of the N-terminal signal peptide structure of the protein, no significant signal peptide cleavage site was observed, indicating that the protein lacked both a signal peptide and a transmembrane region. The amino acid sequence contained an N-glycosylation site, a casein kinase II phosphorylation site, a microsomal C-terminal target signal site, and a manganese and iron superoxide dismutase signal site. The probability of intracytoplasmic localization of the SodB protein was 56.5%, which was analyzed according to the subcellular localization of the protein. The amino acid sequence of the *sodB* gene of *V. alginolyticus* exhibited 98% - 100% homology to other *Vibrio* species, clustering into the same subfamily with *V. parahaem*, indicating a relatively close relationship between them. In the prediction of protein structure, the proportions of α-helix, random coil, β-sheet, and extended strand were 48.45%, 30.41%, 5.67%, and 15.46%, respectively. The similarity to template 1dt0.1.A reached 71.58%. A PTM site analysis revealed the presence of phosphorylation, glycosylation, ubiquitination, sumoylation, acetylation, and methylation modification sites, as well as the absence of lactylation modification sites.

Key words *Vibrio alginolyticus*, Gene cloning, *sodB* gene, Bioinformatics analysis

1 Introduction

Vibrio alginolyticus is a facultative anaerobic bacterium. It is a short rod-shaped bacterium, with a length of approximately 1.4 - 2.6 μm and a width of 0.5 - 0.8 μm. It is devoid of spores and capsules, yet it is equipped with polar and lateral flagella. The optimal growth temperature is 28 ℃, the optimal pH is 7.2, and the highest level of activity is observed when the culture is maintained for 18 h[1-3]. A number of studies have indicated that *V. alginolyticus* can infect a range of animals and humans in the ocean, resulting in a variety of diseases. The pathogen is most likely to cause epidemics when the water temperature is 25 - 35 ℃. It primarily affects marine animals such as shrimp, shellfish, and fish, causing symptoms such as epidermal ulcers, hemorrhages, and black spots, causing significant challenges for the aquaculture industry in the warm waters of the southern part of China[4]. *V. alginolyticus* is a bacterium that is frequently associated with food poisoning and diarrhea in humans. It also causes a range of other diseases, including otitis media and septicemia[5-7]. *V. alginolyticus* is responsible for a wide range of hazards, including vibriosis associated with farmed hybrid grouper in Malaysia[8], mussels and oysters in the Netherlands[9], and *Epinephelus akaara*, *Litopenaeus vannamei*, and *Lutjanus sanguineus* farmed in the southern coastal provinces of China. Consequently, a comprehensive investigation of the pathogenic principles affecting aquatic animals is of paramount importance for the advancement of economic and social development.

Reactive oxygen species (ROS) can be produced not only during the metabolism of microorganisms, but also during the host's immune response to pathogens[10]. It is often observed that inflammation induced by *V. alginolyticus* contributes to the production of large amounts of ROS. *V. alginolyticus* demonstrates the capacity to survive and colonize in the gastrointestinal tract, indicating that it has an effective adaptation to oxidative stress despite being stimulated by higher levels of ROS[11]. The regulation of ROS is influenced by antioxidant enzymes and small molecule antioxidants. Superoxide dismutase (SOD) plays a pivotal role in the removal of ROS[12]. The classification of SOD into three distinct types is dependent upon the presence of specific prosthetic metal cofactors, including manganese superoxide dismutase, iron

Received: February 27, 2024 Accepted: June 12, 2024
Supported by Outstanding Graduate Entering Laboratory Project of College of Fisheries, Guangdong Ocean University; National Natural Science Foundation of China (32073015); Undergraduate Innovation and Entrepreneurship Training Program of Guangdong Ocean University (CXXL2024007); Undergraduate Innovation Team of Guangdong Ocean University (CCTD201802).
△These authors contributed equally to this work.
* Corresponding author. Huanying PANG, PhD., associate professor, research fields: aquatic veterinary medicine.

superoxide dismutase, and copper-zinc superoxide dismutase. These cofactors are encoded by the *sodA*, *sodB*, and *sodC* genes, respectively[13]. In *Pseudomonas aeruginosa*, iron superoxide dismutase plays a more critical role than manganese superoxide dismutase in an oxygen-adequate environment, in its ability to combat the herbicide paraquat and in the synthesis of ceruloplasmin[14]. The *sodB*-deficient mutant displays an exceptionally sensitive response to oxidative stress and a reduced virulence[15]. Nevertheless, there are numerous avenues for further investigation into the role of *sodB* in *V. alginolyticus* that remain unexplored.

Although *sodB* has been demonstrated to be crucial for bacterial persistence and virulence during host infection, only a limited number of studies have been conducted on the role of *sodB* in *V. alginolyticus*. In the present study, the molecular cloning technique was employed to obtain the *sodB* gene of *V. alginolyticus* HY9901, which was then analyzed by bioinformatics tools in order to provide a certain reference basis for in-depth investigation of its function.

2 Materials and methods

2.1 Materials

2.1.1 Strains. The virulent strain HY9901 of *V. alginolyticus* was preserved by the Guangdong Provincial Key Laboratory of Aquatic Animal Disease Control and Healthy Culture[13].

2.1.2 Reagents. The Ex*Taq* DNA polymerase was procured from Takara Biotechnology (Dalian) Co., Ltd. The bacterial genomic DNA extraction kit and DNA gel recovery kit were purchased from Beijing TransGen Biotech Co., Ltd. The remaining reagents were imported or domestically produced and were of an analytically pure quality. The PCR primers were synthesized and sequenced by Invitrogen Shanghai Trading Co., Ltd. The antibiotics were procured from Sigma.

2.2 Methods

2.2.1 Extraction of total DNA from *V. alginolyticus* HY9901. One milliliter of *V. alginolyticus*, which had been cultured overnight, was centrifuged at 12 000 rpm/min, after which the supernatant was removed. Next, 20 μL of Proteinase K and 100 μL of LB11 were added, and the solution was repeatedly blown with a pipette until the bacteria were thoroughly suspended. The solution was then incubated at 55 ℃ for 15 min until it became clear. A precise 20 μL of RNase A was added and thoroughly mixed, and the mixture was then allowed to stand for 2 min. Subsequently, 400 μL of BB11 was added and vortexed for 30 sec. It is possible that transparent gels or white flocs might be produced, but these did not affect the extraction of DNA. The entire solution was transferred to a centrifuge column and subjected to centrifugation at 12 000 rpm for 30 sec. The waste solution was then discarded. Next, 400 μL of CB11 was added, and the mixture was centrifuged at 12 000 rpm for 30 sec. The resulting waste solution was discarded, and the procedure was repeated twice. The solution was subjected to centrifugation at 12 000 rpm for 2 min in order to completely remove WB11. The column was placed in a clean centrifuge tube and left at room temperature for 5 min. It was then added to a preheated (65 ℃) EB solution and left to stand for 2 min before centrifugation at 12 000 rpm for 2 min to elute the DNA. The eluted DNA can be utilized directly for the subsequent experiment or stored at a temperature of −20 ℃.

2.2.2 Cloning of *sodB* gene. A pair of primers was designed according to the sequence of *sodB* gene from *V. alginolyticus*. The upstream primer, designated P1, was ATGGCATTTGAACTACCAGC, while the downstream primer, designated P2, was TTACTTCGCTAGGTTCTCAG. A polymerase chain reaction (PCR) was conducted using the total DNA extracted from *V. alginolyticus* HY9901 as the template. The reaction was conducted under the following conditions: pre-denaturation at 94 ℃ for 5 min; denaturation at 94 ℃ for 30 sec, annealing at 58 ℃ for 30 sec, and extension at 72 ℃ for 40 sec, 33 cycles; and extension at 72 ℃ for 10 min. Following the examination of the PCR products by 1% agarose gel electrophoresis, the gel was cut and recovered using a gel-cutting kit. The recovered fragments were then cloned into the pMD18-T vector, which was named pMD-*sodB*.

2.2.3 Bioinformatics analysis of *sodB* gene of *V. alginolyticus* HY9901. A similarity analysis and homology comparison service for DNA or protein sequences was conducted using the NCBI website (http://blast.ncbi.nlm.nih.gov/Blast.cgi). The DNAMAN 6.0 software was employed for amino acid homology comparison. The ExPASy Proteomics Server (http://ca.expasy.org) was utilized to calculate protein molecular weight (Mw) and make theoretical isoelectric point (pI) predictions. The signal peptide sequences were predicted by online analysis software SignalP 4.0 Server (http://www.cbs.dtu.dk/services/SignalP). The transmembrane structural domains were predicted by TMHMM Server 2.0 (http://www.cbs.dtu.dk/services/TMHMM). The distribution of functional sites in amino acid sequences was predicted by SoftBerry − Psite (http://linux1.softberry.com/berry.phtml?topic=psite&group=programs&subgroup=proloc). The protein structure-function domains were analyzed using InterProScan Sequence Search (http://www.ebi.ac.uk/Tools/InterProScan), while the subcellular localization was predicted using PSORT II Prediction (http://psort.hgc.jp/form2.html). A Phylogenetic tree was constructed using the neighbor-joining method with the Clastal 2.0 and MEGA 5.0 software. A modeling analysis was conducted using the SWISS-MODEL program (http://www.swissmodel.expasy.org/).

3 Results and analysis

3.1 Amplification of *sodB* gene A specific band of approximately 585 bp was successfully obtained by PCR (Fig. 1), which encoded 194 amino acids (AGV17070.1).

3.2 Physicochemical properties of SodB The SodB protein of *V. alginolytici* HY9901 was analyzed using the ExPASy software. The results indicate that the protein has a total of 2 981 atoms, with a molecular structure formula of $C_{987}H_{1451}N_{249}O_{291}S_3$, a theoretical molecular weight of 21.557 05 kDa, a theoretical pI value of 4.95, an instability coefficient of 28.52 (stable), a fat coeffi-

cient of 77.06, a total average hydrophilicity of −0.238, and that the protein is hydrophobic in general. The protein in question does not contain selenocysteine (Sec), pyrrole lysine (Pyl), and has a molar extinction coefficient of 50 420 mol/cm at 280 nm. The total number of acidic amino acids (Asp + Glu) is 24, and the total number of basic amino acids (Arg + Lys) is 12, with methionine (Met) at the N-terminus. The half-life of expression in yeast and *E. coli* is greater than 20 and 10 h, respectively, while the half-life of expression in mammalian reticulocytes in *in vitro* culture is found to be 30 h.

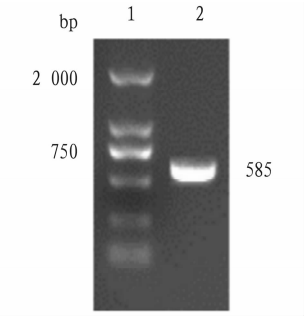

NOTE 1. DNA marker DL2000; 2. PCR products of *sodB* gene.

Fig. 1 Amplification of *sodB* gene

3.3 Sequence analysis of SodB Upon analysis of the SodB amino acid sequence using the SignalP 4.0 Server, it was determined that the N-terminal signal peptide structure was not present, indicating that the signal peptide is not present in the sequence. The TMHMM Server 2.0 program predicted that the protein would not cross the region of the cell membrane. The SoftBerry – Psite program identified a binding site for manganese and iron superoxide dismutase signals (158 – 165 aa), a casein kinase II phosphorylation site (46 – 49 aa), an N-glycosylation site (73 – 76 aa), and a microsomal C-terminal target signaling site (109 – 111 aa) (Fig. 2). The predicted subcellular localization of the protein, based on the available evidence, indicated that SodB was most likely to be located in the cytoplasm with a likelihood of 56.5%. This was followed by the nucleus with a likelihood of 30.4%, the mitochondria with a likelihood of 8.7%, and finally the Golgi complex with a likelihood of 4.3%.

3.4 Homology and evolutionary analysis of *sodB* A BLAST analysis revealed that the *sodB* gene of *V. alginolyticus* exhibited high homology with the *sodB* gene of other *Vibrio* species. Among these, it exhibited the highest homology with the amino acid sequence of the *sodB* gene of *V. parahaemolyticus* (99%). Furthermore, multiple sequence similarity comparisons indicated that the *sodB* gene in *Vibrio* is highly conserved (Fig. 3).

The deduced amino acid sequences of SodB protein were employed to construct a phylogenetic tree with other microorganisms using the neighbor-joining method with MEGA 5.0 software. The results demonstrated that the SodB proteins of *V. alginolyticus* HY9901 clustered into the same subfamily with *V. parahaemolyticus*, indicating a closer kinship (Fig. 4). This finding corroborates the results of the traditional classification of morphologic and biochemical characteristics.

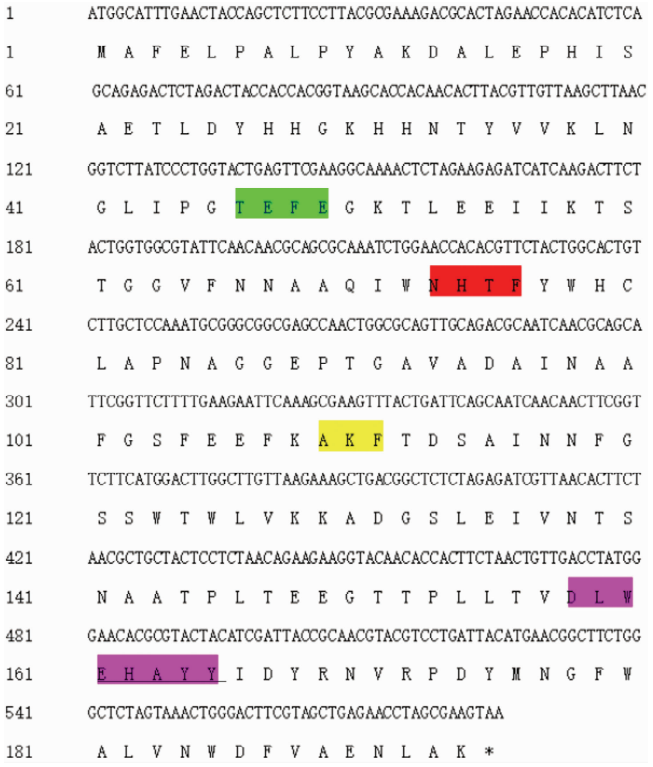

NOTE Terminators are indicated by *; green sections represent casein kinase II phosphorylation sites; red sections represent N-glycosylation sites; yellow sections represent microsomal C-terminal target signaling sites; pink sections represent manganese and iron superoxide dismutase signaling sites.

Fig. 2 Nucleotides of the *sodB* gene and their encoded amino acid sequences

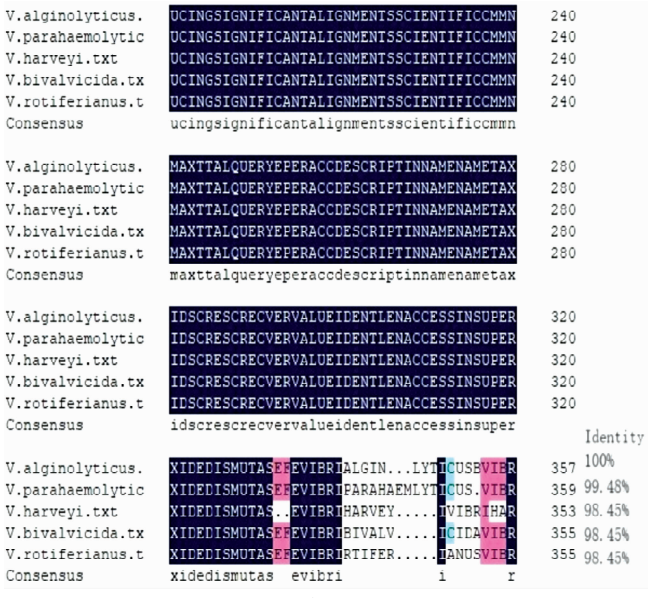

NOTE *Vibrio alginolyticus* (EEZ 83613.1); *V. parahaemolyticus* (MDG 2998714.1); *V. harveyi* (WP 038898599.1); *V. bivalvicida* (WP 054961506.1); *V. rotiferianus* (WP 071234641.1).

Fig. 3 Homology comparison of amino acid sequences derived from *sodB* gene

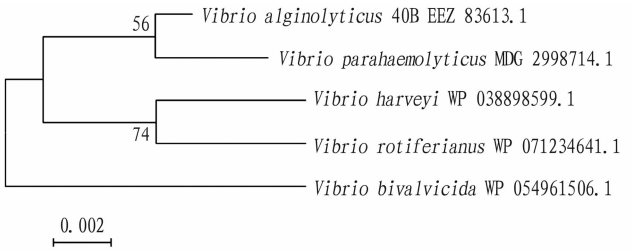

Fig.4 SodB amino acid phylogenetic tree constructed based on the NJ method

3.5 Functional domains, secondary and tertiary structure prediction of SodB The SMART program revealed the existence of two principal functional domains within SodB (Fig.5). In the secondary structure prediction, the α-helix was identified with a frequency of 48.45%, while the random coil, extended strand, and β-sheet were observed with the frequency of 30.41%, 15.46%, and 5.67%, respectively (Fig.6).

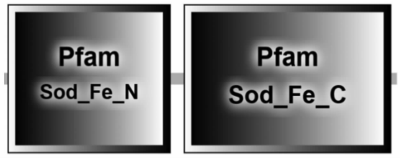

Fig.5 Functional domains of SodB

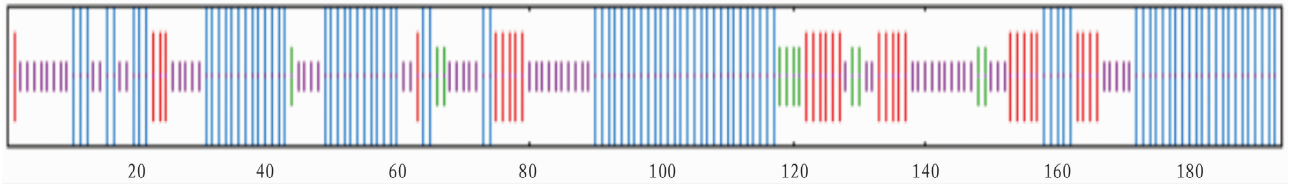

NOTE Blue: α-helix; Purple: random coil; Red: extended strand; Green: β-sheet.

Fig.6 Secondary structure prediction of SodB

The Swiss-Model program employed an automated process for generating three-dimensional structural models of proteins. This process began with the input of the amino acid sequence of SodB. The program then searched for homologous proteins that can be used as templates, ultimately generating a three-dimensional structural model of the single subunit of SodB (Fig.7).

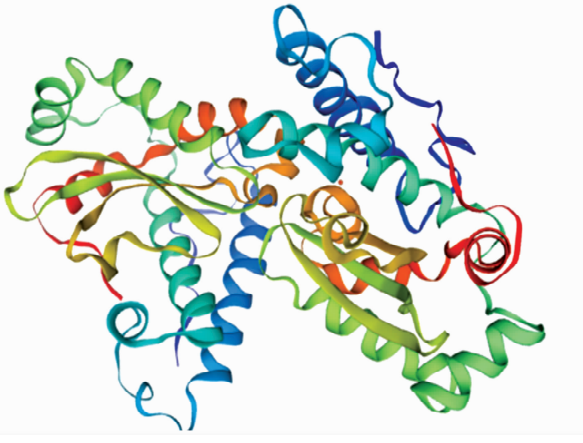

NOTE Template: 1dt0.1.A; Similarity: 71.58%.

Fig.7 Tertiary structure prediction of SodB

3.6 Protein-protein interaction (PPI) network of SodB Among the PPI networks, it can be observed that the proteins adjacent to the SodB protein included YbeY, Rnc, SucD, ANP67689.1, ANP64874.1, ANP67214.1, RplM, RpsO, RpmG, and Rpsl (Fig.8).

3.7 Analysis of SodB PTM modification sites The amino acid sequence of SodB was submitted to automatic analysis using the programs Musite Deep (https://www.musite.net/) and FSL-Kla (http://kla.zbiolab.cn/). This analysis revealed the presence of phosphorylation, glycosylation, ubiquitination, sumoylation, acetylation, and methylation modification sites, as well as the absence of lactylation modification sites.

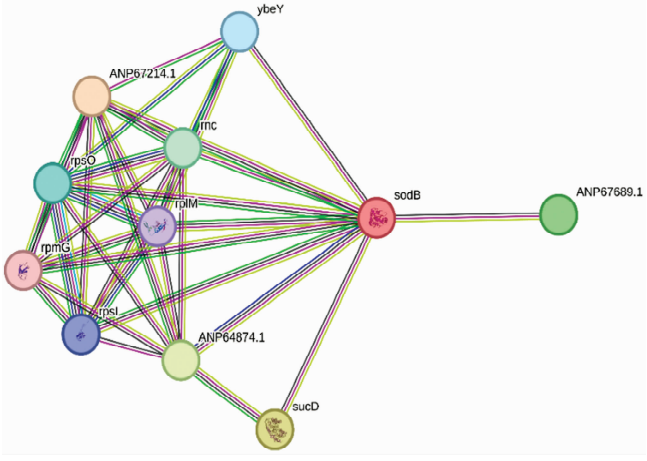

Fig.8 PPI network of SodB

4 Discussion

In this study, the amino acid sequence of the *sodB* gene of *V. alginolyticus* HY9901 was utilized for a comprehensive and comparative analysis. This analysis included a variety of parameters, such as secondary structure, tertiary structure, transmembrane region, hydrophilicity, and protein-protein network interactions. The structure of the N-terminal signal peptide of the amino acid sequence of SodB was predicted. The results of this analysis showed that no obvious signal peptide cleavage site existed and that no signal peptide existed.

SOD is a metalloenzyme that is widely distributed in living organisms. It catalyzes the disproportionation of superoxide anions, specifically removing excess superoxide anions, and maintaining the balance of oxygen free radicals[16]. SOD activity is regarded as a crucial indicator for evaluating antioxidant properties[17-19]. A

number of studies have demonstrated that an increase in ROS stimulates biofilm formation, while SOD plays a pivotal role in the removal of ROS. In particular, it has been observed that mutation of the bacterial *sodB* gene reduces the activity of the SOD enzyme and diminishes the pathogenicity of the bacteria in mice[15]. Following a series of comparative analyses, the *sodB* gene of *Vibrio* is identified as exhibiting a high degree of similarity to the amino acid sequences of other bacteria, with similarities ranging from 98% to 100%. The deletion of the *sodB* gene in *V. alginolyticus* has been observed to result in a reduction in the organism's resistance to free radicals in the external environment. Conversely, an increase in ROS has been shown to facilitate the formation of biofilms. The deletion of *sodB* in *V. alginolyticus* results in the inhibition of SOD activity and an increase in biofilm formation. It is presumed that the inhibition of SOD activity increases intracellular oxidative stress of *sodB*, which in turn further enhances biofilm formation[15,20]. The results of the bioinformatics analysis of the *sodB* gene may provide support for exploring the role of *sodB* gene in the physiology and pathogenicity of *V. alginolyticus*, as well as for the development of vaccines.

PTMs play a pivotal role in regulating cellular processes. For instance, phosphorylation is involved in signal transduction and cell cycle regulation[21], while acetylation is implicated in transcriptional regulation and cell metabolism[22]. Glycosylation, on the other hand, is essential for cell adhesion and protein folding[23]. However, when a protein undergoes multiple post-translational modifications (PTMs) simultaneously, these modifications interact with each other, forming a complex called PTM co-modification[24-25]. Among the various modification processes, both reversible protein phosphorylation and lysine acetylation represent conserved and universal regulatory mechanisms in bacteria. The disturbances of phosphorylation and lysine acetylation are transmitted through direct interactions[26]. Acetylation is a process that reduces the response of proteins to phosphorylation. It typically occurs on proteins that are subject to covalent ubiquitination, which regulates other protein-modifying enzymes and forms macromolecular complexes[22]. For instance, acetylation of K^{11} on histone H2B inhibits phosphorylation of S^{10}[26-27]. Previous studies have demonstrated that phosphorylation exerts a pivotal influence on the subsequent ubiquitination process. The degree of phosphorylation of ubiquitinated proteins is relatively stable, and a comparison of the conservation of ubiquitination sites between phosphorylated and non-phosphorylated proteins reveals no significant difference between them. The findings indicate a trend towards global crosstalk, with phosphorylation occurring more frequently prior to ubiquitination[28]. H_2O_2-induced ASK1 activity can be inhibited by PRMT5 methylation of ASK1 at the Arg-89 site, which in turn promotes the interaction between ASK1 and Akt and increases phosphorylation at the Ser-83 site, thereby inhibiting apoptosis[29].

References

[1] PANG HY, ZHOU ZJ, DING Y, *et al.* Molecular cloning and bioinformatics analysis of T3SS chaperone escort protein VscO from *Vibrio alginolyticus*[J]. Biotechnology Bulletin, 2014(6): 155-161. (in Chinese).

[2] DING SY, HOU LY, YU CY, *et al.* Research progress on pathogenic mechanism of marine Vibrios[J]. Occupation and Health, 2019, 35(7): 984-989. (in Chinese).

[3] LI JY. Molecular mechanism of *Vibrio alginolyticus* infection in *Litopenaeus vannamei* and study on bacteriophage control[D]. Guangzhou: South China Agricultural University, 2023. (in Chinese).

[4] WANG FQ, SUN YZ, REN LH, *et al.* Research progress on the main pathogenic *Vibrio* affecting aquatic animals in mariculture[J]. Chinese Fishery Quality and Standards, 2018, 8(2): 49-56. (in Chinese).

[5] WAGNER KR, CRICHTON EP. Marine vibrio infections acquired in Canada[J]. Canadian Medical Association Journal, 1981, 124(4): 435.

[6] LI XC, XIANG ZY, XU XM, *et al.* Endophthalmitis caused by *Vibrio alginolyticus*[J]. Journal of Clinical Microbiology, 2009, 47(10): 3379-3381.

[7] ARDI N, OZYURT M. Case report: Otitis due to *Vibrio alginolyticus*[J]. Mikrobiyoloji Bulteni, 2004, 38(1-2): 145-148.

[8] MOHAMAD N, MOHD ROSELI FA, AZMAI MNA, *et al.* Natural concurrent infection of *Vibrio harveyi* and *V. alginolyticus* in cultured hybrid groupers in Malaysia[J]. Journal of Aquatic Animal Health, 2019, 31(1): 88-96.

[9] KAMPELMACHER E, VAN NOORLE JANSEN LM, MOSSEL D, *et al.* A survey of the occurrence of *Vibrio parahaemolyticus* and *V. alginolyticus* on mussels and oysters and in estuarine waters in the Netherlands[J]. Journal of Applied Bacteriology, 1972, 35(3): 431-438.

[10] RAY PD, HUANG BW, TSUJI Y. Reactive oxygen species (ROS) homeostasis and redox regulation in cellular signaling[J]. Cellular Signalling, 2012, 24(5): 981-90.

[11] CAI S, CHENG H, PANG H, *et al.* AcfA is an essential regulator for pathogenesis of fish pathogen *Vibrio alginolyticus*[J]. Veterinary Microbiology, 2018(213): 35-41.

[12] MIAO L, CLAIR DK. Regulation of superoxide dismutase genes: Implications in disease[J]. Free Radical Biology & Medicine, 2009, 47(4): 344-356.

[13] CHEN YY. Study on the function and regulation of accessory colonization factor AcfA of *Vibrio alginolyticus* to SOD, Flg and Dct[D]. Zhanjiang: Guangdong Ocean University, 2020. (in Chinese).

[14] HASSETT DJ, SCHWEIZER HP, OHMAN DE. *Pseudomonas aeruginosa sodA* and *sodB* mutants defective in manganese-and iron-cofactored superoxide dismutase activity demonstrate the importance of the iron-cofactored form in aerobic metabolism[J]. Journal of Bacteriology, 1995, 177(22): 6330-6337.

[15] BAKSHI CS, MALIK M, REGAN K, *et al.* Superoxide dismutase B gene (*sodB*)-deficient mutants of *Francisella tularensis* demonstrate hypersensitivity to oxidative stress and attenuated virulence[J]. Journal of Bacteriology, 2006, 188(17): 6443-6448.

[16] NIEDERHOFFER EC, NARANJO CM, BRADLEY KL, *et al.* Control of *Escherichia coli* superoxide dismutase (*sodA* and *sodB*) genes by the ferric uptake regulation (fur) locus[J]. Journal of Bacteriology, 1990, 172(4): 1930-1938.

[17] LI YL, LEI K, XU X, *et al.* Protective Effect of *Bacillus subtilis* B10 against hydrogen peroxide-induced oxidative stress in a murine macrophage cell line[J]. International Journal of Agriculture & Biology, 2013, 15(5): 927-932.

[18] AIASSA V, BARNES AI, ALBESA IJB, *et al.* Resistance to ciprofloxacin by enhancement of antioxidant defenses in biofilm and planktonic *Proteus mirabilis*[J]. Biochemical and Biophysical Research Communications, 2010, 393(1): 84-88.

[19] CHEN X, ZHANG E, FANG L, *et al.* Repair effects of exogenous SOD on *Bacillus subtilis* against gamma radiation exposure[J]. Journal of Environmental Radioactivity, 2013(126): 259-263.

[20] CHEN Y, WU F, PANG H, *et al.* Superoxide dismutase B (sodB), an important virulence factor of *Vibrio alginolyticus*, contributes to antioxidative stress and its potential application for live attenuated vaccine[J].

Fish and Shellfish Immunology, 2019, 89: 354 – 360.
[21] UBERSAX JA, FERRELL JE. Mechanisms of specificity in protein phosphorylation[J]. Molecular Cell Biology, 2007, 8(7): 530 – 541.
[22] CHOUDHARY C, KUMAR C, GNAD F, *et al.* Lysine acetylation targets protein complexes and co-regulates major cellular functions[J]. Science, 2009, 325(5942): 834 – 840.
[23] OHTSUBO K, MARTH JD. Glycosylation in cellular mechanisms of health and disease[J]. Cell, 2006, 126(5): 855 – 867.
[24] WANG LN. Computing identification and bioinformatics analyses of lysine post-translational modification sites[D]. Nanchang: Nanchang University, 2018. (in Chinese).
[25] GRAY VE, LIU L, NIRANKARI R, *et al.* Signatures of natural selection on mutations of residues with multiple posttranslational modifications [J]. Molecular Biology and Evolution, 2014, 31(7): 1641 – 1645.
[26] VAN NOORT V, SEEBACHER J, BADER S, *et al.* Cross-talk between phosphorylation and lysine acetylation in a genome-reduced bacterium [J]. Molecular Systems Biology, 2012, 8(1): 571.
[27] AHN SH, DIAZ RL, GRUNSTEIN M, *et al.* Histone H2B deacetylation at lysine 11 is required for yeast apoptosis induced by phosphorylation of H2B at serine 10[J]. Molecular Cell, 2006, 24(2): 211 – 220.
[28] SWANEY DL, BELTRAO P, STARITA L, *et al.* Global analysis of phosphorylation and ubiquitylation cross-talk in protein degradation[J]. Nature Methods, 2013, 10(7): 676 – 682.
[29] CHEN M, QU X, ZHANG Z, *et al.* Cross-talk between Arg methylation and Ser phosphorylation modulates apoptosis signal – regulating kinase 1 activation in endothelial cells[J]. Molecular Biology of the Cell, 2016, 27(8): 1358 – 1366.

(From page 38)

Table 1 Comparison of main technical and economic indicators

No.	Project		Underpass bridge project "small trucks pass underneath, large trucks pass above"	Trestle bridge project "small trucks rolling on ground, large trucks rolling on bridge"	Trestle bridge project "large trucks rolling on ground, small trucks rolling on bridge"
1	Investment (10 000 yuan)	Bridge body	1 500	1 500	2 250
		Bridge earthwork	367.0	0	0
		Road reconstruction	31.5	257.3	190.0
		Total	1 898.5	1 757.3	2 440.0
2	Small truck efficiency change		Higher	Higher	Higher
3	Small truck transportation cost change		Lower	Higher	Lower
4	Construction period//d		90	40	40
5	Idling period//d		90	0	40
6	Degree of road congestion		Mild	Mild	Mild
7	Difficulty level of vehicle scheduling		Easy	Easy	Easy
8	Ranking by comparison		2	1	3

References

[1] CAI BJ, SONG CS, WEI YL. Using box steel assembly roads and culverts to solve the problem of limited transportation flow in open-pit mines[J]. Open-pit Mine Technology, 2013(7): 106 – 110. (in Chinese).
[2] ZHANG LT. Comparison of the relocation location of the crushing station in the open-pit mine[J]. Open-pit Mining Technology, 2018(3): 42 – 45. (in Chinese).
[3] DONG SB. Optimization scheme of south band transportation system of Anjialing open pit mine[J]. Open-pit Mine Technology, 2019(5): 54 – 57. (in Chinese).
[4] XU CP, LIU QX. Analysis on the cooperation mode of the end-side transportation system of Huaneng Yimin Open-pit Mine[J]. Open-pit Mining Technology, 2009(4): 16 – 18. (in Chinese).
[5] LI HF. Lifting and transformation of raw coal and stripping transportation system in Xiwan Open Pit Coal Mine[J]. Open-pit Mine Technology, 2021(4): 86 – 89. (in Chinese).
[6] LIU Y, LEI ZY, WANG PL, *et al.* Application of pithead interchange steel trestle in Xiwan Open-pit Coal Mine[J]. Open-pit Mining Technology, 2018(6): 10 – 13. (in Chinese).
[7] CAI BJ, SONG CS, WEI YL. Using box steel assembly roads and culverts to solve the problem of limited transportation flow at the east end of Yimin Open-pit Mine[J]. Open-pit Mine Technology, 2013(10): 37 – 35. (in Chinese).
[8] LIU YM. Interchange underpass bridge project[J]. Shanxi Construction, 2011(2): 182 – 183. (in Chinese).